

# Origin of line broadening in the electronic absorption spectra of conjugated polymers: Three-pulse-echo studies of MEH-PPV in toluene

Gregory D. Scholes, Delmar S. Larsen, and Graham R. Fleming

*Department of Chemistry, University of California, Berkeley, California 94720*

*and Physical Biosciences Division, Lawrence Berkeley National Laboratory, Berkeley, California 94720-1460*

Garry Rumbles

*Centre for Electronic Materials and Devices, Department of Chemistry, Imperial College of Science, Technology, and Medicine,  
Exhibition Road, London SW7 2AY, United Kingdom*

Paul L. Burn

*Dyson Perrins Laboratory, Oxford University, Oxford OX1 3QY, United Kingdom*

(Received 23 November 1999)

Integrated three-pulse stimulated echo peak shift data are compared for *N,N*-bis-dimethylphenyl-2,4,6,8-perylenetetracarboxyl diamide and poly[2-(2'-ethylhexyloxy)-5-methoxy-1,4-phenylenevinylene] (MEH-PPV) in toluene solvent. These two molecules represent a model probe of solvation dynamics and a prototypical soluble, electroluminescent conjugated polymer, respectively. The results indicate that it is inappropriate to describe the linear absorption spectrum of MEH-PPV as being primarily inhomogeneously broadened. Conformational disorder along the polymer backbone gives rise to an ensemble of polyene electronic oscillators that are strongly coupled to each other. As a consequence, fluctuations in the electronic energy gap on a time-scale of 50-fs derive primarily from bath-mediated exciton scattering. The data reported here provide an explanation for the broad, structureless electronic absorption of MEH-PPV. This interpretation provides a valuable insight into the nature of the initial photoexcited state, and the efficient population of the emissive state.

## I. INTRODUCTION

Since their discovery, there has been intensive study of organic conjugated polymers owing to the promise of applications in electroluminescent devices (e.g., optical displays and light-emitting diodes) and optical switches.<sup>1-3</sup> They have the advantages of favorable processing characteristics and interesting semiconducting properties, which may be tuned by chemical tailoring. In recent years there has been considerable progress toward the development and understanding of electroluminescent devices based on poly(arylenevinylene), such as the material investigated in the present work, poly[2-(2'-ethylhexyloxy)-5-methoxy-1,4-phenylenevinylene] (MEH-PPV). Detailed aspects of their photo-physics that have significant implications to their function, however, remain elusive and controversial.

A significant determinant of the electro-optic response of conjugated polymers is conformational disorder. It is widely accepted that, because energy barriers for rotation around single bonds in conjugated chains are of the same order as  $kT$ , there are breaks in the conjugation over the length of the polymer.<sup>4-9</sup> These are referred to as "conformational subunits" of the polymer chain. Each of these subunits has a corresponding unbroken  $\pi$  system, which we refer to either as the conjugation length or the delocalization length. Qualitative explanations of solvatochromism and thermochromism have been suggested by models based upon an inhomogeneous distribution of conjugation lengths, and hence excitation energies. In such work the optical properties of conju-

gated polymers have been connected to an effective conjugation length.

Our goal in these ongoing studies is to develop a picture which rationalizes the microscopic chemical model describing absorbing units of the disordered conjugated backbone with the mesoscopic optoelectric and optical properties. Models of conformational disorder based on barriers for conformational motion typically predict that conjugation lengths are short relative to that limited by the molecular weight of the polymer. It is often taken to be a corollary that the absorption line shape is determined by an inhomogeneous distribution of absorptions corresponding to these conformational subunits.<sup>5,6</sup> Such a concept is incongruous with estimations of "effective" conjugation length obtained through analysis of properties such as the static third-order optical susceptibility  $\gamma$ ,<sup>10-13</sup> or the saturation of such properties with oligomer molecular weight.<sup>14-16</sup> Single molecule studies of "one-step" photobleaching of MEH-PPV also suggest that electronic interactions extend along much of the length of the polymer chain.<sup>17</sup> Furthermore, it is difficult to understand electroluminescent exciton formation, or the observation of conduction or semiconductorlike properties, in the rigid constraints of such a line-shape model. In this regard, the interactions that couple conformational subunits along the one-dimensional nanostructure are of considerable interest.

Fitting the electronic absorption spectra of conjugated polymers is of considerable interest owing to the possibility of obtaining information regarding the nature of the elementary excitations and the role of Coulomb correlations in the

$\pi$ -conjugated system.<sup>18</sup> Conjugated polymers are of particular interest because they appear to belong to an intermediate correlation regime.<sup>19</sup> However, although such information is contained in the linear absorption spectrum, it cannot be extracted unambiguously from line-shape analysis. This is because linear spectroscopies are insensitive to the time scales of fluctuations of the electronic energy gap induced by interaction of the chromophore with complex condensed phase environments, and therefore—even in the case of a two-level system—cannot differentiate between homogeneous and inhomogeneous broadening arising from coupling of the electronic transition to the bath (electron-phonon coupling).<sup>20,21</sup> On the other hand, nonlinear spectroscopies are capable of providing a line-shape function, or spectral density, which reveals all the time scales of the dephasing processes that are coupled to the electronic transition.<sup>22–24</sup> In the case of molecular aggregates or semiconductor nanostructures, the analysis of line shape is even more complicated because the interactions between electronic transitions lead to a renormalization of transition energies and the emergence of additional dephasing mechanisms.<sup>25–30</sup>

Here we report on an investigation of the origin of the electronic absorption line shape function for MEH-PPV in toluene using the three-pulse stimulated echo peak shift (3PEPS) method. Time-resolved four-wave-mixing experiments have been employed successfully in the past to study microscopic relaxation and dephasing processes in complex systems.<sup>31</sup> In contrast to the usual integrated two-pulse echo (2PE) measurement, where one time delay—the coherence time—is varied, the integrated 3PE signal has a dynamic range from femtoseconds to nanoseconds, owing to the introduction of an additional time delay: the population time. The peak shift protocol provides a way of reducing this information contained in the two time delays. Previously, this method has provided incisive information on the time scales and mechanism of polar and nonpolar solvation,<sup>32–37</sup> as well as energy-transfer dynamics in weakly coupled molecular aggregates.<sup>38,39</sup> In order to understand better the nonlinear response of MEH-PPV, we contrast it to that of the chromophore *N,N*-bis-dimethylphenyl-2,4,6,8-perylenetetracarboxyl diamide (PERY). The structures of these two chromophores are shown in Fig. 1. PERY is nondipolar and nonionic, and is a model probe of solvation dynamics.<sup>37</sup> The solvation dynamics of such a dilute two-level chromophore system are dominated by fluctuations and reorganization arising from electron-nuclear coupling. Conjugated polymers, however, represent a quite different class of chemical systems. While conjugated polymers do interact with the surrounding bath in essentially the same way as a model “two-level” chromophore (i.e., PERY), we expect that their nonlinear response contains additional information regarding dynamics associated with interactions within the extensive  $\pi$ -electron system of the polymer backbone.<sup>12,40–44</sup> Thus it is not clear what to expect for the case of MEH-PPV in terms of the origin of the line shape for electronic linear absorption. We suggest on the basis of the observations reported herein that the simple terms “homogeneous” and “inhomogeneous” fail to describe adequately the origin of the absorption line shapes of conjugated polymers because of the multiple time scales of the fluctuations contributing to con-

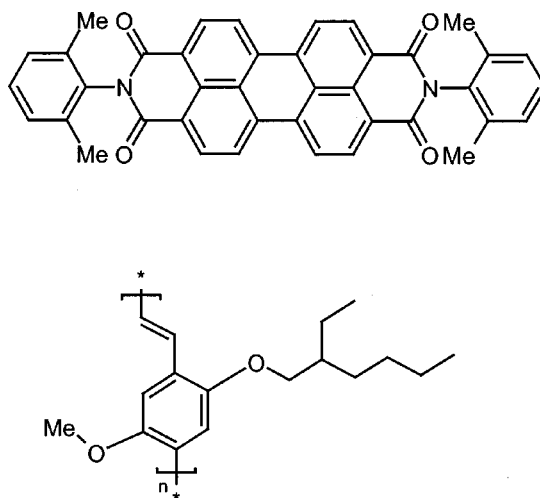


FIG. 1. Molecular structures of the model probe chromophore for solvation dynamics, PERY, and the soluble electroluminescent conjugated polymer MEH-PPV.

formational disorder, electronic scattering, and electron-phonon coupling.

## II. EXPERIMENTAL SECTION

The 3PEPS method was described in detail previously.<sup>32,34</sup> Here we used a tuneable optical parametric amplifier (OPA) pumped by a regeneratively-amplified Ti:sapphire laser (Coherent Mira-RegA) as the excitation source. Nearly transform-limited pulses of 40-fs duration and repetition rate of 250 kHz were used, centered at a wavelength of 530 nm. The output from the OPA was split into three beams (1, 2, and 3 in Fig. 2) of equal polarization,

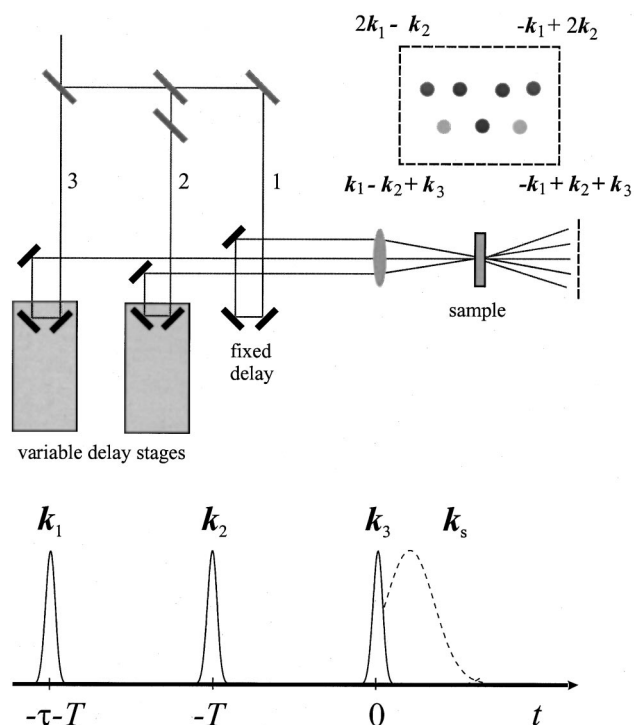


FIG. 2. Experimental arrangement and pulse sequence for the 3PEPS experiment. See the text for details.

intensity (each with a pulse energy of  $<10$  nJ at the sample), and experiencing equal dispersion from the optical components. Beams 2 and 3 can be delayed, while the fixed-delay beam 1 was chopped. The beams were aligned in an equilateral triangle geometry ( $\sim 1$ -cm side) and focused into the sample using a 20-cm focal length fused silica singlet lens. This experimental setup is shown in Fig. 2. Signals were spatially isolated and recorded using diodes and lock-in detection. No unusual power dependence of the signal could be observed for pulse energies in the range 2–15 nJ. Data were also collected at a later date using a repetition rate of 60 kHz and longer pulses (50–60-fs full width at half maximum). Consistent results were obtained.

Toluene (spectroscopic grade) was obtained from Aldrich Chemical Company. PERY was purchased from Aldrich. Solutions of PERY in toluene were filtered to remove insoluble impurities. Samples were flowed through a 0.1-mm path-length cell at optical densities of approximately 0.1 or less and a temperature of 293 K. By examining the absorption spectrum we have excluded any significant contributions to the signals from interpolymer associations.

NMR spectra were recorded on a Gemini 200 MHz spectrometer. IR spectra were recorded on a Perkin-Elmer Paragon 1000 Fourier transform infrared spectrometer. UV-visible spectra were carried out on a Perkin-Elmer Lambda 14P spectrometer. Gel permeation chromatography (GPC) was carried out using PLgel 20- $\mu$ m Mixed-A columns [(600+300)-mm lengths, 7.5-mm diameter] from Polymer Laboratories calibrated with polystyrene narrow standards [ $M_p = (1300-15.4) \times 10^6$ ] in tetrahydrofuran with toluene as flow marker. The tetrahydrofuran was degassed with helium and pumped at a rate of 1 mL/min at  $22^\circ\text{C} \pm 1^\circ\text{C}$ .

Poly[2-(2'-ethylhexyloxy)-5-methoxy-1,4-phenylenevinylene] was prepared by the addition of potassium *t*-butoxide in dry tetrahydrofuran (0.95 M, 20 mL) to a vigorously stirred solution of 1,4-bis-chloromethyl-2-(2'-ethylhexyloxy)-5-methoxybenzene (1.0 g 3.0 mmol) in dry tetrahydrofuran (80 mL) at room temperature under nitrogen. The reaction mixture was stirred for 24 h at room temperature and was then poured onto methanol (500 mL). The resultant red precipitate was filtered and washed well with water. The precipitate was redissolved in tetrahydrofuran (100 mL), filtered through a sinter, and then precipitated by addition to methanol (500 mL). The precipitate was collected and dried under vacuum to give poly[2-(2'-ethylhexyloxy)-5-methoxy-1,4-phenylenevinylene] ( $\approx 0.40$  g, 45%),  $\lambda_{\text{max}}(\text{CH}_2\text{Cl}_2)/\text{nm}$  334 and 505;  $\nu_{\text{max}}(\text{KBr})/\text{cm}^{-1}$  962(C=CH) and 3055 (C=CH);  $\delta H$  (200 MHz;  $\text{CDCl}_3$ ) 0.83–1.13 ( $2 \times \text{CH}_3$ ), 1.20–1.96 (CH and  $\text{CH}_2$ ), 3.81–4.14 ( $\text{OCH}_3$  and  $\text{OCH}_2$ ), 6.57–6.67, 6.97–7.31, and 7.41–7.68 (Ar H and vinyl H); GPC,  $\bar{M}_w = 4.9 \times 10^5$ , and  $\bar{M}_n = 1.1 \times 10^5$ .

The electronic absorption and photoluminescence spectra of the sample are shown in Fig. 3. The absorption peaks at 490 nm and the emission maximum is at 555 nm. The sample exhibits a photoluminescence quantum yield of  $0.33 \pm 0.09$ , determined relative to rhodamine 101, and a lifetime of  $380 \pm 30$  ps, measured using time-correlated single photon counting. The radiative lifetime is therefore approximately 1 ns, indicative of a fully allowed radiative transition.

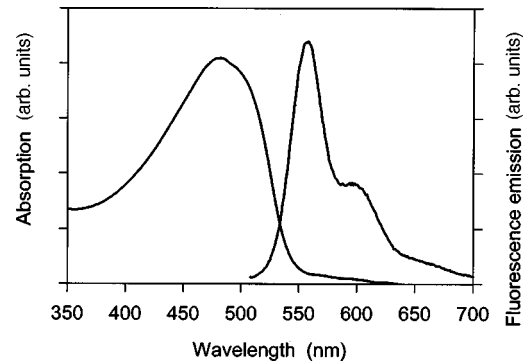


FIG. 3. Absorption and photoluminescence spectra of MEH-PPV in toluene.

### III. RESULTS

To describe the key features of the 3PEPS measurement, it is usual<sup>24,32</sup> to separate the electronic energy gap between ground  $g$  and excited  $e$  states into its average value  $\langle \varepsilon_{eg}^k \rangle$  for site  $k$ , and a fluctuating term which is an incisive dynamical probe of the local environment,  $\delta \varepsilon_{eg}(t)$ :

$$\varepsilon_{eg}^k(t) = \langle \varepsilon_{eg}^k \rangle + \delta \varepsilon_{eg}(t). \quad (1)$$

As described elsewhere,<sup>24,32,34</sup> the integrated three-pulse echo signal  $S(T, \tau)$  is given by Eq. (2), with  $\tau$  being the time delay between the first two pulse (the coherence period),  $T$  the time delay between pulses 2 and 3 (the population period), and  $t$  the time evolution of the nonlinear polarization after the third pulse:

$$S(T, \tau) = \int_0^\infty dt |R(t, T, \tau)|^2. \quad (2)$$

For a two-level system with resonant excitation, there are four unique contributions to the response function  $R(t, T, \tau)$  which generate a third-order polarization in the  $-\mathbf{k}_1 + \mathbf{k}_2 + \mathbf{k}_3$  (3PE) phase-matching direction. Having a nonzero peak shift (denoted  $\tau^*$ ), that is, a value of  $\tau$  corresponding to the maximum of  $S(T, \tau)$  for a fixed  $T$ , relies on the presence of the fluctuating contribution to the electronic energy gap  $\delta \varepsilon_{eg}(t)$ . The 3PEPS experiment provides detailed information on the electronic energy gap correlation function, and is directly sensitive to the solvation dynamics, but not to population decay. Moreover, if the inhomogeneous width is comparable to the dynamical width, then the observation of a nonzero asymptotic peak shift at long population times provides definitive evidence of an inhomogeneous contribution to the optical absorption spectrum.<sup>21,32,38,45,46</sup> Additional details of the 3PEPS experiment are provided in the Appendix.

The integrated three-pulse stimulated echo signal intensity  $S(T, \tau)$  versus the first time delay  $\tau$  for various population times  $T$  for both PERY and MEH-PPV in toluene are shown in Fig. 4 for the signal directions  $\mathbf{k}_1 - \mathbf{k}_2 + \mathbf{k}_3$  and  $-\mathbf{k}_1 + \mathbf{k}_2 + \mathbf{k}_3$ , at population times  $T = 0, 20,$  and  $48$  fs. Both probe chromophores have a high initial peak shift of 18 fs, indicative of weak coupling between their respective electronic transitions and the bath. This is typical for nonpolar solvation, and has also been observed in benzene and carbon tetrachloride solvents.<sup>37</sup> Note that the precise value of the initial peak shift is also dependent also on the laser pulse width and

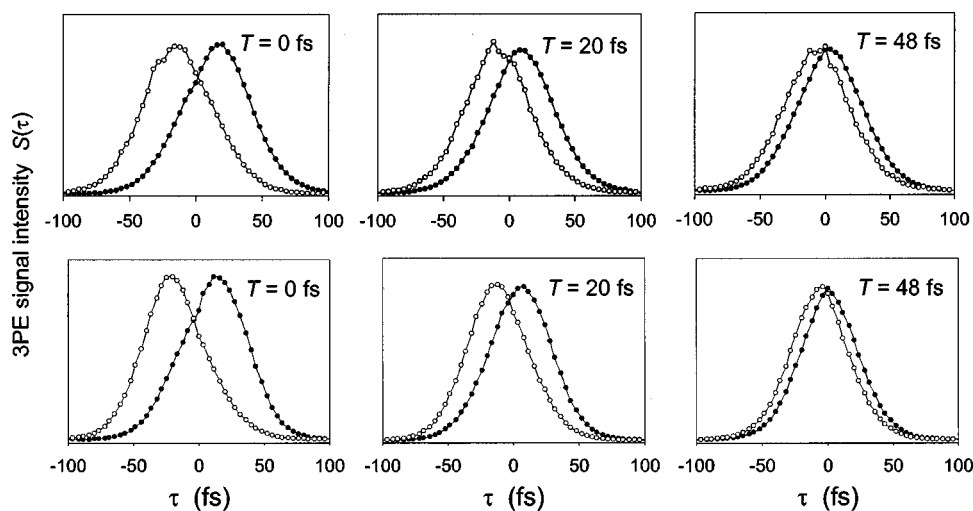


FIG. 4. Integrated three-pulse stimulated echo (3PE) signal intensities  $S(T, \tau)$  vs the first time delay  $\tau$  for population times  $T = 0, 20,$  and  $48$  fs, for both PERY (upper panels) and MEH-PPV (lower panels) in toluene. Open circles are the data for the signal direction  $\mathbf{k}_1 - \mathbf{k}_2 + \mathbf{k}_3$  and filled circles are for the signal direction  $-\mathbf{k}_1 + \mathbf{k}_2 + \mathbf{k}_3$ . The peak shift is defined as half the separation between the maxima of these two signals.

solvation time scales. Meaningful direct comparison of the PERY 3PE data  $S(T, t)$  for  $T = 20$  and  $48$  fs to that of MEH-PPV is complicated by the strong oscillations in the PERY 3PEPS data, which are due to coherently excited vibrational modes.

A better contrast between the time scales of fluctuations that lead to dephasing is evident from inspection of the 3PEPS data (peak shift  $\tau^*$  versus population time  $T$ ) for each probe chromophore. These data were obtained by taking half the separation between the 3PE peaks for the two signal directions—hence obviating the necessity to determine precisely  $\tau = 0$ —and are plotted in Fig. 5 (diamonds), along with the simulated data (solid line) for both PERY and MEH-PPV in toluene. The simulations are discussed below. The PERY 3PEPS data decay quite slowly, attaining a peak shift of  $1.5$  fs at a population time of  $6$  ps. The marked and persistent oscillations of the coherently excited intramolecular vibrations are indicative of weak coupling between chromophore and bath. In contrast, the MEH-PPV peak shift data decay rapidly, attaining a peak shift of  $1.5$  fs at a population time of only  $100$  fs. Bearing in mind that the peak shift is

approximately proportional to the electronic energy gap correlation function,<sup>32,34</sup> and therefore to time scales of bath fluctuations that are coupled to the electronic transition, a comparison of the PERY and the MEH-PPV data suggests that the origin of the fluctuations which are coupled to the electronic transitions is fundamentally different for each of these two chromophores.

The 3PEPS data were simulated using the usual procedure<sup>34</sup> in order to obtain the electronic energy-gap correlation function  $M(t)$ , which provides details of the time scales of bath fluctuations. In general, for a dilute probe molecule such as PERY in this way we obtain an estimate of the electronic transition energy correlation function [Eq. (3)], that describes the fluctuations at a single site, in this case a chromophore  $k$ . The time scales of the bath fluctuations contained in  $M(t)$  are representative of the solvent bath, and can generally be retrieved using any dilute probe chromophore:

$$M_{kk}(t) \equiv \langle \delta\omega^k(t) \delta\omega^k(0) \rangle. \quad (3)$$

The 3PEPS data for PERY in toluene were found to

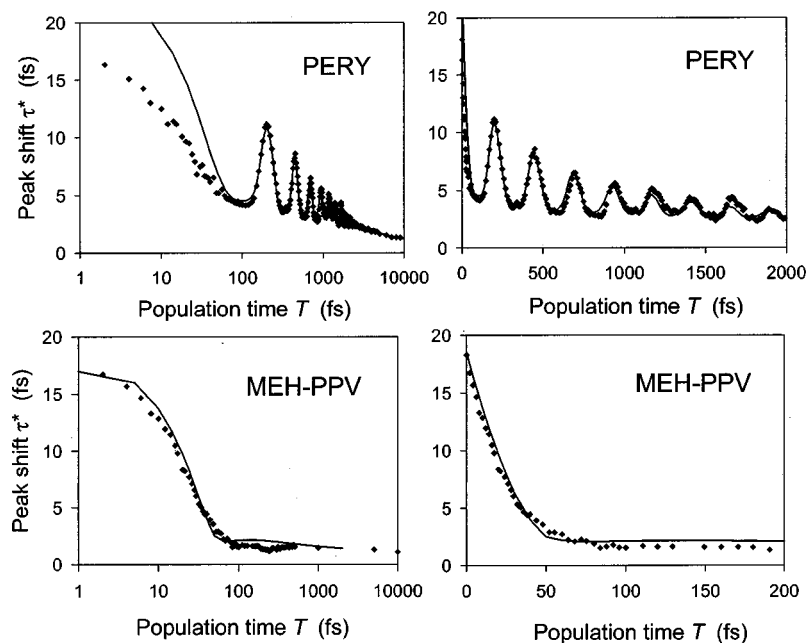


FIG. 5. Three pulse stimulated echo peak shift (3PEPS) vs population time for PERY in toluene (upper panels) and MEH-PPV in toluene (lower panels). Note that the scales on the abscissae of the plots in the right-hand panels differ.

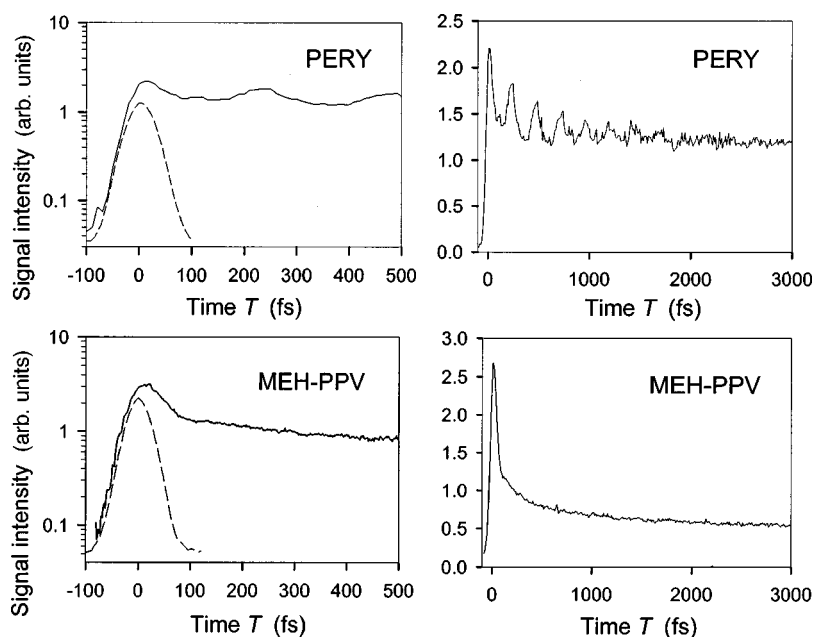


FIG. 6. Transient grating (TG) data for both PERY and MEH-PPV in toluene. In the transient grating experiment, the first two pulses ( $\mathbf{k}_1$  and  $\mathbf{k}_2$ ) arrive at the sample simultaneously and generate a population grating, which is probed by the third pulse  $\mathbf{k}_3$ . The TG signal intensity exhibits a sharp peak for delay times less than the autocorrelation width of the laser pulse owing to non-rephasing contributions to the response functions. For reference, this is compared with the 3PE signals for  $T=48$  fs in the direction  $\mathbf{k}_1 - \mathbf{k}_2 + \mathbf{k}_3$  (dashed lines).

be best fit by  $M(t)$  with a Gaussian component  $\lambda_1 \exp[-(t/\tau_1)^2]$ ,  $\lambda_1 = 80 \text{ cm}^{-1}$  and  $\tau_1 = 80$  fs, and three exponential components  $\lambda_j \exp(t/\tau_j)$ , with  $\lambda_2 = 5 \text{ cm}^{-1}$  and  $\tau_2 = 650$  fs;  $\lambda_3 = 25 \text{ cm}^{-1}$  and  $\tau_3 = 3.0$  ps; and  $\lambda_4 = 5 \text{ cm}^{-1}$  and  $\tau_4 = 120$  ps. Note the small coupling strengths  $\lambda_j$  characteristic of nonpolar solvation. The coherently excited intramolecular vibrations were simulated as damped cosines  $\lambda_i \exp(-t/\tau_i) \cos(\omega_i t + \phi_i)$ , with  $\lambda_5 = 45 \text{ cm}^{-1}$ ,  $\tau_5 = 820$  fs,  $\omega_5 = 139 \text{ cm}^{-1}$ , and  $\phi_5 = 0.15$  rad, and  $\lambda_6 = 24 \text{ cm}^{-1}$ ,  $\tau_6 = 712$  fs,  $\omega_6 = 278 \text{ cm}^{-1}$ , and  $\phi_6 = 0.0$  rad. The Stokes shift for PERY in toluene was experimentally determined to be  $373 \text{ cm}^{-1}$ .

The 3PEPS data for MEH-PPV in toluene (over the range  $T=0-5$  ps) were modeled using the same response functions as for the dilute chromophore case. The energy-gap correlation function can be well represented by a sum of exponentials  $\lambda_j \exp(t/\tau_j)$ , with  $\lambda_1 = 700 \text{ cm}^{-1}$  and  $\tau_1 = 50 \pm 20$  fs;  $\lambda_2 = 120 \text{ cm}^{-1}$  and  $\tau_2 = 400 \pm 50$  fs; and  $\lambda_3 = 250 \text{ cm}^{-1}$  and  $\tau_3 = 15$  ps. The time constant  $\tau_3$  was not determined with high accuracy, but represents a contribution from either static inhomogeneity or a slow spectral diffusion process. Such a small residual inhomogeneity may be the result of photo-oxidation of the sample, or it may be due to slight aggregation of the polymers.<sup>47</sup> On the other hand, it could represent the ‘‘red emitting’’ states of the polymer, which would be an interpretation consistent with recent single-molecule studies.<sup>48</sup> The errors in the coupling strengths are estimated to be approximately  $\pm 10\%$ . The coupling strengths were constrained such that their sum equals half the Stokes shift estimated from the difference in the peak maxima of the absorption and emission spectra:  $\lambda = 1070 \text{ cm}^{-1}$ . The different time scales obtained from analysis of the PERY 3PEPS data compared to that for MEH-PPV—despite the same solvent bath present in each case—suggests that the fluctuations of the electronic energy gaps, and hence the line broadening mechanisms, for these chromophores are derived from distinctly different physical processes.

We need to be convinced that the rapid decay component

in the peak shift of MEH-PPV is not due to exciton-exciton annihilation during the population period.<sup>49</sup> To this end, in Fig. 6 we report transient grating (TG) data for both PERY and MEH-PPV in toluene. In the transient grating experiment, the first two pulses arrive at the sample simultaneously and generate a population grating, which is probed by the scattering of the third pulse. The TG signal intensity exhibits a sharp peak for delay times less than the autocorrelation width of the laser pulse, owing to ultrafast inertial solvation and nonrephasing contributions to the response functions.<sup>34</sup> There is no evidence in the MEH-PPV TG data of any significant contribution from a fast decay component that would suggest that the dephasing actually arises from exciton-exciton annihilation. However, the longer time dynamics of the TG decay are highly nonexponential, which could be ascribed to either exciton-exciton annihilation or exciton transport to states that absorb outside the spectral bandwidth of the laser.<sup>50,51</sup>

#### IV. DISCUSSION

The nonlinear response of polyenes and perfect conjugated polymers constitutes a complex many-body problem owing to the strong correlation effects characteristic of these electronically delocalized systems.<sup>42,43,52</sup> For a realistic treatment of the experimental data we need to consider the nonlinear response of a conjugated polymer with conformational disorder. In the most simplistic model, the absorption spectrum can be modeled as a linear combination of absorption line shapes of perfect polyenes, representing noninteracting conformational subunits. In this case, the absorption spectrum would be described as being inhomogeneously broadened. This would be clearly evident in the 3PEPS data as an asymptotic residual peak shift;<sup>45,46</sup> in other words,  $\lambda_1$  would be small compared to  $\lambda_3$ . However, it is clear that this is not the case; the rapid decay of the MEH-PPV peak shift toward zero suggests that there is minimal persistent energetic disorder. This was quantified in the simulations by the very large  $\lambda_1$  and short  $\tau_1$ . Hence, in order to describe properly

linear and nonlinear response of MEH-PPV in a consistent framework, we must consider a minimal model that accounts for the interaction between the primary excitations representing absorbing subunits along the polymer chain.

A model involving an inhomogeneous set of coupled two-level systems, each consisting of optically coupled ground and excited states (semiconductor Bloch equations and elaborations thereof) has been used successfully to model nonlinear optical properties of semiconductors (e.g., optical Stark effect and two-pulse echo data).<sup>28,29,53–56</sup> The 3PE, however, involves propagation through an additional time  $T$ , under a diagonal density operator, which is interpreted macroscopically as a population grating comprised of ground- and excited-state molecules.<sup>24,32,34</sup> A more sophisticated theory for four-wave-mixing signals for molecular aggregates was recently developed by Mukamel and co-workers,<sup>25,26,44</sup> which includes the effects of two-exciton states (i.e., the  $A_g$  electronic oscillators), static disorder, and coupling to a phonon bath of arbitrary spectral density. It is equally applicable to a semiconductor band-gap model or to molecular excitons. A clear physical picture can be obtained from the electronic-oscillator analysis developed by these workers.<sup>57,58</sup> In the work of Meier *et al.*,<sup>43</sup> it was suggested that only two electronic oscillators need to be considered explicitly ( $B_u$  and  $A_g$ ), all others being excited off-resonance. However, the nonlinear response still contains contributions additional to that reminiscent of a two-level system. These arise because the primary  $A_g$  oscillator is optically active via a two-photon transition at the excitation frequency. Hence, as described by Yaron and Silbey,<sup>11</sup> for example, the minimal model for the nonlinear response of a conjugated polymer is cast in terms of Liouville space pathways that involve three intermediate states  $|0\rangle \Rightarrow |1\rangle \Rightarrow |2\rangle \Rightarrow |3\rangle \Rightarrow |0\rangle$ , with  $\Rightarrow$  indicating a transition moment connection. Here  $|0\rangle$  is the ground state,  $|1\rangle$  and  $|3\rangle$  are one-exciton states ( $B_u$  electronic oscillators), and  $|2\rangle$  can be the ground state, a one-exciton state, or a two-exciton state ( $A_g$  electronic oscillator). According to Yaron and Silbey,<sup>11</sup> terms where  $|2\rangle$  is either the ground state or a one-exciton state represent exciton migration terms and dominate the nonlinear response owing to cancellations involving the two-exciton intermediate state contributions.

From that work, as well as from 3PEPS studies of photosynthetic light-harvesting complexes,<sup>38,45</sup> it is clear that significant additional contributions to the nonlinear response arise owing to interactions  $V_{k,k'}$  between chromophores (proximate electronic oscillators labeled  $k$  and  $k'$ ). When  $V_{k,k'}$  is nonzero (e.g., the case of MEH-PPV), fluctuations of a distinctly different nature from those which lead to dephasing in a perfect polyene are introduced owing to intersubunit exciton hopping and ground-state bleaching. These contributions to the response diminish the apparent distribution of static disorder (inhomogeneous width) by increasing the overall dephasing. In other words, in the nonlinear response, the distribution of  $\varepsilon_{eg}^k$  are coupled via  $V_{k,k'}$ , thus introducing rapid fluctuations over the spectral distribution of conformational subunits. Moreover, in conjugated polymers there is also significant static disorder and/or stochastic fluctuations in the coupling  $V_{k,k'}$  itself.<sup>7</sup>

To see what this means for the absorption line shape (linear response) of a conjugated polymer (e.g., MEH-PPV)

compared to a two-level system coupled to a harmonic bath (e.g., PERY), here we deduce a physical picture based on our interpretation of the 3PEPS data. The linear polarization is given by  $P^{(1)}(t) = \int_0^\infty dt_1 R^{(1)}(t_1) \varepsilon(t-t_1)$ , where the response function for a two-level system (such as PERY) is given by

$$R_{TLS}^{(1)}(t) = \langle i | \mu_m |^2 [J(t) - J^\dagger(t)] \rangle_{\text{disorder}}, \quad (4)$$

with

$$J(t) = \exp[-i\omega_m - g(t)], \quad (5)$$

where  $g(t)$  is the line-shape function, directly related to the electronic energy gap correlation function via  $g(t) = \int_0^t d\tau \int_0^\tau d\tau' M(\tau')$ .<sup>24</sup> The ensemble average over static disorder which may arise from extremely slow fluctuations of the bath, for example in a rigid polymer glass solvent, is written explicitly. This is the inhomogeneous contribution to the line shape. The fast fluctuations of the bath, arising from stochastic random fluctuations in the bath of phonon oscillators,<sup>22–24</sup> contribute to the homogeneous line shape through  $g(t)$ .

For a molecular aggregate system, however, we cannot make a simple separation between the molecular eigenstates and the bath dynamics. The linear-response function is given by

$$R_{agg}^{(1)}(t) = \left\langle i \sum_{m,n} \mu_m^{(1)} \mu_n^{(1)} [G_{mn}(t) - G_{mn}^\dagger(t)] \right\rangle_{\text{disorder}}, \quad (6)$$

where  $G_{mn}(t)$  is the function described in Ref. 26 that describes the interplay between one-exciton Green's functions and the collective bath coordinate. The logical starting point to determine the one-exciton Green's functions is a Hamiltonian describing the  $\pi$ -electron system in terms of the alternating single and double bonds, for example, the Pariser-Parr-Pople or INDO/SCI Hamiltonians which have been shown to be useful for describing the key properties of conjugated polyenes.<sup>59,60</sup> Conformational disorder must be included at this level in order to determine ensemble average properties of the conjugated polymer.<sup>61</sup> A significant effect of this disorder is to generate a number of eigenstates that lie close in energy and loosely correspond to absorptions into spatially separated conformational subunits along the polymer chain. These eigenstates, labeled  $m, n, \dots$ , can be used as the basis for a Hamiltonian that will be used to calculate the equations of motion for the system.

A clear difference between the two-level system and the conjugated polymer is now apparent: the diagonal and off-diagonal static disorders have a significant effect on the nature of these eigenstates.<sup>7,62</sup> This suggests that, analogously, some of the fast bath fluctuations that are coupled to the instantaneous eigenstates of the polymer will have a dynamic effect on the electronic energy gaps at the level of the electronic eigenstates. The nuclear motions effecting this should be primarily associated with intramolecular motions, and some evidence that this is the case for epitaxial polydiacetylene films has been reported by Pham *et al.*<sup>63</sup> These workers also reported an excitonic dephasing time of 52 fs.

Thus while the line broadening in the absorption spectrum of a two-level system is introduced by coupling of the bath

fluctuations to the electronic energy gap, that for a molecular aggregate is determined by exciton population relaxation as well as pure dephasing involving both electronic and nuclear interactions. This pure dephasing may be viewed as bath-mediated scattering over the eigenstates. A further detail that may have significance as a dephasing mechanism in conjugated polymers is the effect of bath-mediated fluctuations in  $V_{k,k'}$ . In the present paper we describe these effects phenomenologically. This is accomplished by separating the electronic energy gap correlation function of Eq. (3) into two distinct contributions,<sup>54</sup> fluctuations at a single site  $M_{kk}(t)$  and a contribution arising from intersite scattering  $M_{kk'}(t)$ :

$$M_{kk}(t) \equiv \langle \delta\omega^k(t) \delta\omega^k(0) \rangle, \quad (7a)$$

$$M_{kk'}(t) \equiv \langle \delta\omega^{k'}(t) \delta\omega^k(0) \rangle. \quad (7b)$$

The single-site fluctuations of Eq. 7(a) are indicative of solvation dynamics, and owing to the dissimilarity of the MEH-PPV 3PEPS data from those of PERY (both in toluene), we conclude that it is the various dephasing mechanisms contributing intersite correlations [Eq. 7b] that dominate the MEH-PPV nonlinear response. These are related to the exciton migration terms identified by Yaron and Silbey.<sup>11</sup> Noting the rapid decay of the 3PE peak shift of MEH-PPV to 1.5 fs at a population time  $T=100$  fs suggests that an averaging over the conformational subunits occurs primarily on a 50-fs time-scale. This precludes any significant static inhomogeneous distribution of excitation energies in the absorption line shape, at least in the region of the absorption spectrum resonant with the laser pulse spectrum. Moreover, the observation that this contribution dominates the 3PEPS signal—in striking contrast to the PERY data—provides firm evidence that  $V_{k,k'}$  are significant compared to solute-solvent couplings. Thus, although there certainly is a distribution of conformational subunits along an ensemble of polymer backbones, which in turn provide a distribution of localized excitation energy gaps, analysis of the 3PEPS data reported here suggests that the *subunits are strongly coupled to each other*. This is an important result implied by the 3PEPS measurement, and is independent of the model used for the correlation function.

The fast dephasing time observed for MEH-PPV, significantly shorter than the fluorescence lifetime, indicates that ergodicity is satisfied, and that therefore there exists a relationship between the absorption line shape and the Stokes shift between absorption and photoluminescence; via fluctuation-dissipation. This provides support for our model of the electronic energy-gap time-dependent correlation function insofar as the total coupling strength to the fluctuations equals half the Stokes shift. Hence our model describes the 3PEPS data, the absorption line shape, and the large Stokes shift of the photoluminescence spectrum. There are additional dissipative processes, seen in the transient grating data, that represent irreversible exciton migration processes and account for the relaxation of the excited-state population to the distribution of states from which photoluminescence takes place.<sup>48,51</sup>

We suggest that the results we have reported here provide the bridge between linear spectroscopic observables (e.g., the absorption maximum and Stokes shift) and understanding

properties that scale critically with the polymer length (e.g., cubic optical nonlinearity). The absorption maximum of long-chain polyene oligomers redshifts with the average number of double bonds  $N$  in the sample. However, this bathochromic shift saturates quickly with increasing  $N$ . In other words, the absorption maximum is not a sensitive indicator of the average  $N$  in a polymer sample. On the other hand, the enhancement of nonlinear properties, such as cubic optical nonlinearity, with  $N$  is remarkable.<sup>14</sup> Here we have reported an observation that the interaction between the set of primary electronic oscillators representing conformational subunits (arising from conformational disorder) in MEH-PPV is significant. As a consequence, we do not expect the scaling of linear and nonlinear responses to be isomorphic, primarily because of the sensitivity of the nonlinear response to electron correlation.

## V. CONCLUSIONS

In the present report we investigated the origin of the line shape for electronic linear absorption of a prototypical soluble, electroluminescent conjugated polymer, poly[2-(2'-ethylhexyloxy)-5-methoxy-1,4-phenylenevinylene] (MEH-PPV) in toluene solvent. Integrated three-pulse stimulated echo peak shift data were compared for  $N,N$ -bis-dimethylphenyl-2,4,6,8-perylenetetracarboxyl diamide (PERY), a model two-level probe of solvation dynamics and MEH-PPV. We suggested that the simple terms “homogeneous” and “inhomogeneous” fail to describe adequately the absorption line shapes of conjugated polymers because the time scales of fluctuations contributing to, and arising from, conformational disorder, electronic scattering, and electron-phonon coupling are complex.

The picture we presented here is summarized as follows. Conformational disorder along the polymer backbone gives rise to an ensemble of polyene electronic oscillators that are strongly coupled to each other by Coulomb interactions. As a consequence, fluctuations in the electronic energy gap, observed here to have a characteristic relaxation time scale of 50 fs, derive primarily from bath-mediated exciton scattering. The electron-phonon couplings at each conformational subunit are small—characteristic of nonpolar solvation—as demonstrated by comparison of the MEH-PPV data with that for PERY. The linear absorption line shape of MEH-PPV is significantly affected by the interplay between the fluctuations controlling conformational disorder and their impact on the electronic eigenstates. The data reported here suggest strongly that these fluctuations—arising from coupled electronic and nuclear interactions—are fast on the experimental time scale, since the decay of the peak shift indicates that there is very little static inhomogeneity (within the laser pulse bandwidth) that persists for times comparable to the fluorescence lifetime. Furthermore, simulation of the peak shift decay for MEH-PPV in toluene, based on the phenomenological correlation functions of Eqs. 7, reproduces the Stokes shift for photoluminescence and assigns its origin to fluctuations mediated by the coupled electronic oscillators. This provides an explanation for the broad, structureless electronic absorption of MEH-PPV and possibly many other well-solvated conjugated polymers. This interpretation provides a valuable insight into the nature of the initial photo-

excited state, and the efficient population of the emissive state.

### ACKNOWLEDGMENTS

This work was supported by grants from the National Science Foundation (G.R.F.) and EPSRC (G.R.). Professor Shaul Mukamel is gratefully acknowledged for helpful discussions. Minhaeng Cho (Korea University) is thanked for enlightening discussions. Dr. Kaoru Ohta (Fleming Group) is acknowledged for assistance with the experimental work.

### APPENDIX

Three pulse echo peak shift (3PEPS) spectroscopy provides a useful reduction of the information content of the time-integrated three pulse echo (3PE) signal. The 3PE signal is generated by the resonant interaction of three optical pulses with an ensemble of chromophores. The first pulse  $\mathbf{k}_1$  creates a coherence between ground and excited states. After a time delay  $\tau$ , the second pulse  $\mathbf{k}_2$  converts this coherence to a population which undergoes spectral diffusion and possibly other dynamic processes for a time  $T$ . The final pulse  $\mathbf{k}_3$  converts this population to a coherence that may generate an echo in the  $\mathbf{k}_s = -\mathbf{k}_1 + \mathbf{k}_2 + \mathbf{k}_3$  signal direction. In the 3PEPS experiment we simultaneously measure a signal in the  $\mathbf{k}'_s = \mathbf{k}_1 - \mathbf{k}_2 + \mathbf{k}_3$  signal direction, which corresponds to the pulse sequence  $\mathbf{k}_2, \mathbf{k}_1, \mathbf{k}_3$ . We do this to determine the peak shift  $\tau^*$ —half the difference between the values of  $\tau$  at the maxima of  $\mathbf{k}_s$  and  $\mathbf{k}'_s$ —to greater precision.

The 3PEPS experiment provides details of the time scales (or spectrum) and amplitude of fluctuations of the electronic energy gap [Eq. (1)]. Fluctuations as distinct as site energy

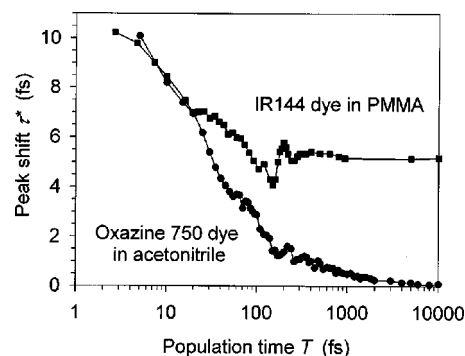


FIG. 7. Comparison of 3PEPS data for a probe chromophore in a liquid (oxazine 750 in acetonitrile) with a probe chromophore in a rigid polymer glass (IR 144 in polymethylmethacrylate). See the Appendix.

differences that persist for times significantly longer than the experimental time window, static inhomogeneity, compared to the rapid fluctuations that lead to “homogeneous” line broadening can be clearly differentiated. This is facilitated by the enormous dynamic range of the 3PEPS data; from a few fs up to hundreds of ps. As an example, a comparison of 3PEPS data for a probe chromophore in a liquid (oxazine 750 in acetonitrile) with a probe chromophore in a rigid polymer glass (IR144 in polymethylmethacrylate, PMMA) is shown in Fig. 7. The 3PEPS data for oxazine 750 decay to an asymptotic value of 0 fs according to the time scales of fluctuations in the acetonitrile bath. This is indicative of homogeneous line broadening. In contrast, the asymptotic value of the peak shift data for IR144 in PMMA is approximately 5 fs. Such a nonzero asymptotic peak shift is a direct measure of the distribution of static inhomogeneity of IR144 excitation energies in the polymer matrix.

- <sup>1</sup>J. H. Burroughes, D. D. C. Bradley, A. R. Brown, R. N. Marks, K. Mackay, R. H. Friend, P. L. Burns, and A. B. Holmes, *Nature (London)* **347**, 539 (1990).
- <sup>2</sup>R. H. Friend, R. W. Gymer, A. B. Holmes, J. H. Burroughes, R. N. Marks, C. Taliani, D. D. C. Bradley, D. A. Dos Santos, J. L. Bredas, M. Logdlund, and W. R. Salaneck, *Nature (London)* **397**, 121 (1999).
- <sup>3</sup>Q. B. Pei, G. Yu, C. Zhang, Y. Yang, and A. J. Heeger, *Science* **269**, 1086 (1995).
- <sup>4</sup>J. Cornil, D. A. dos Santos, X. Crispin, R. Silbey, and J. L. Bredas, *J. Am. Chem. Soc.* **120**, 1289 (1998).
- <sup>5</sup>B. E. Kohler and I. D. W. Samuel, *J. Chem. Phys.* **103**, 6248 (1995).
- <sup>6</sup>B. E. Kohler and J. C. Woehl, *J. Chem. Phys.* **103**, 6253 (1995).
- <sup>7</sup>M. Schreiber and S. Abe, *Synth. Met.* **55**, 50 (1993).
- <sup>8</sup>K. S. Schweizer, *J. Chem. Phys.* **85**, 1156 (1986).
- <sup>9</sup>S. N. Yaliraki and R. J. Silbey, *J. Chem. Phys.* **104**, 1245 (1996).
- <sup>10</sup>S. Abe, M. Schreiber, W. P. Su, and J. Yu, *Phys. Rev. B* **45**, 9432 (1992).
- <sup>11</sup>D. Yaron and R. Silbey, *Phys. Rev. B* **45**, 11 655 (1992).
- <sup>12</sup>D. Yaron, *Phys. Rev. B* **54**, 4609 (1996).
- <sup>13</sup>S. Kishino, Y. Ueno, K. Ochiai, M. Rikukawa, K. Sanui, T. Kobayashi, H. Kunugita, and K. Ema, *Phys. Rev. B* **58**, R13 430 (1998).
- <sup>14</sup>I. D. W. Samuel, I. Ledoux, C. Dhenaut, J. Zyss, H. H. Fox, R. R. Schrock, and R. J. Silbey, *Science* **265**, 1070 (1994).
- <sup>15</sup>S. Tretiak, V. Chernyak, and S. Mukamel, *Phys. Rev. Lett.* **77**, 4656 (1996).
- <sup>16</sup>S. Mukamel, A. Takahashi, H. X. Wang, and G. Chen, *Science* **266**, 250 (1994).
- <sup>17</sup>D. A. Vanden Bout, W. T. Yip, D. H. Hu, D. K. Fu, T. M. Swager, and P. F. Barbara, *Science* **277**, 1074 (1997).
- <sup>18</sup>M. Chandross, S. Mazumdar, M. Liess, P. A. Lane, Z. V. Vardeny, M. Hamaguchi, and K. Yoshino, *Phys. Rev. B* **55**, 1486 (1997).
- <sup>19</sup>Z. Shuai, J. L. Bredas, A. Saxena, and A. R. Bishop, *J. Chem. Phys.* **109**, 2549 (1998).
- <sup>20</sup>G. R. Fleming and M. H. Cho, *Annu. Rev. Phys. Chem.* **47**, 109 (1996).
- <sup>21</sup>G. R. Fleming, S. A. Passino, and Y. Nagasawa, *Philos. Trans. R. Soc. London, Ser. A* **356**, 389 (1998).
- <sup>22</sup>Y. J. Yan and S. Mukamel, *J. Chem. Phys.* **89**, 5160 (1988).
- <sup>23</sup>Y. J. Yan and S. Mukamel, *Phys. Rev. A* **41**, 6485 (1990).
- <sup>24</sup>S. Mukamel, *Principles of Nonlinear Spectroscopy* (OUP, New York, 1995).
- <sup>25</sup>T. Meier, V. Chernyak, and S. Mukamel, *J. Chem. Phys.* **107**, 8759 (1997).



- <sup>26</sup>V. Chernyak, W. M. Zhang, and S. Mukamel, *J. Chem. Phys.* **109**, 9587 (1998).
- <sup>27</sup>V. M. Axt and S. Mukamel, *Rev. Mod. Phys.* **70**, 145 (1998).
- <sup>28</sup>W. Schafer, D. S. Kim, J. Shah, T. C. Damen, J. E. Cunningham, K. W. Goossen, L. N. Pfeiffer, and K. Kohler, *Phys. Rev. B* **53**, 16 429 (1996).
- <sup>29</sup>H. Haug and S. W. Koch, *Quantum Theory of the Optical and Electronic Properties of Semiconductors*, 3rd ed. (World Scientific, Singapore, 1990).
- <sup>30</sup>R. Binder and S. W. Koch, *Prog. Quantum Electron.* **19**, 307 (1995).
- <sup>31</sup>Y. R. Shen, *The Principles of Nonlinear Optics* (Wiley, New York, 1984).
- <sup>32</sup>M. H. Cho, J. Y. Yu, T. H. Joo, Y. Nagasawa, S. A. Passino, and G. R. Fleming, *J. Phys. Chem.* **100**, 11 944 (1996).
- <sup>33</sup>W. P. Deboeij, M. S. Pshenichnikov, and D. A. Wiersma, *Chem. Phys. Lett.* **253**, 53 (1996).
- <sup>34</sup>T. H. Joo, Y. W. Jia, J. Y. Yu, M. J. Lang, and G. R. Fleming, *J. Chem. Phys.* **104**, 6089 (1996).
- <sup>35</sup>E. T. J. Nibbering, D. A. Wiersma, and K. Duppen, *Chem. Phys.* **183**, 167 (1994).
- <sup>36</sup>X. J. Jordanides, M. J. Lang, X. Y. Song, and G. R. Fleming, *J. Phys. Chem. B* **103**, 7995 (1999).
- <sup>37</sup>D. S. Larsen, K. Ohta, and G. R. Fleming, *J. Chem. Phys.* **111**, 8970 (1999).
- <sup>38</sup>J. Y. Yu, Y. Nagasawa, R. van Grondelle, and G. R. Fleming, *Chem. Phys. Lett.* **280**, 404 (1997).
- <sup>39</sup>M. Yang and G. R. Fleming, *J. Chem. Phys.* **111**, 27 (1999).
- <sup>40</sup>S. Abe, M. Schreiber, and W. P. Su, *Synth. Met.* **57**, 4004 (1993).
- <sup>41</sup>G. J. Blanchard, J. P. Heritage, A. C. Vonlehmen, M. K. Kelly, G. L. Baker, and S. Etemad, *Phys. Rev. Lett.* **63**, 887 (1989).
- <sup>42</sup>T. Meier and S. Mukamel, *Phys. Rev. Lett.* **77**, 3471 (1996).
- <sup>43</sup>T. Meier, S. Tretiak, V. Chernyak, and S. Mukamel, *Phys. Rev. B* **55**, 4960 (1997).
- <sup>44</sup>W. M. Zhang, T. Meier, V. Chernyak, and S. Mukamel, *J. Chem. Phys.* **108**, 7763 (1998).
- <sup>45</sup>Y. Nagasawa, J. Y. Yu, M. H. Cho, and G. R. Fleming, *Faraday Discuss* **108**, 23 (1997).
- <sup>46</sup>Y. Nagasawa, S. A. Passino, T. Joo, and G. R. Fleming, *J. Chem. Phys.* **106**, 4840 (1997).
- <sup>47</sup>T.-Q. Nguyen, V. Doan, and B. J. Schwartz, *J. Chem. Phys.* **110**, 4068 (1999).
- <sup>48</sup>D. H. Hu, J. Yu, and P. F. Barbara, *J. Am. Chem. Soc.* **121**, 6936 (1999).
- <sup>49</sup>M. van Burgel, D. A. Wiersma, and K. Duppen, *J. Chem. Phys.* **102**, 20 (1995).
- <sup>50</sup>R. Kersting, U. Lemmer, R. F. Mahrt, K. Leo, H. Kurz, H. Bassler, and E. O. Gobel, *Phys. Rev. Lett.* **70**, 3820 (1993).
- <sup>51</sup>T. Kobayashi, *Synth. Met.* **54**, 75 (1993).
- <sup>52</sup>J. L. Bredas, C. Adant, P. Tackx, and A. Persoons, *Chem. Rev.* **94**, 243 (1994).
- <sup>53</sup>M. Wegener, D. S. Chemla, S. Schmittrink, and W. Schafer, *Phys. Rev. A* **42**, 5675 (1990).
- <sup>54</sup>S. Schmitt-Rink, S. Mukamel, K. Leo, J. Shah, and D. S. Chemla, *Phys. Rev. A* **44**, 2124 (1991).
- <sup>55</sup>S. Schmitt-Rink and D. S. Chemla, *Phys. Rev. Lett.* **57**, 2752 (1986).
- <sup>56</sup>M. Lindberg, R. Binder, and S. W. Koch, *Phys. Rev. A* **45**, 1865 (1992).
- <sup>57</sup>S. Tretiak, V. Chernyak, and S. Mukamel, *Chem. Phys. Lett.* **259**, 55 (1996).
- <sup>58</sup>S. Mukamel, S. Tretiak, T. Wagersreiter, and V. Chernyak, *Science* **277**, 781 (1997).
- <sup>59</sup>H. Fukutome, *J. Mol. Struct.: THEOCHEM* **188**, 377 (1989).
- <sup>60</sup>J. Cornil, D. Beljonne, R. H. Friend, and J. L. Bredas, *Chem. Phys. Lett.* **223**, 82 (1994).
- <sup>61</sup>G. D. Scholes and G. R. Fleming, *J. Phys. Chem. B* **104**, 1854 (2000).
- <sup>62</sup>H. Fidder, J. Knoester, and D. A. Wiersma, *J. Chem. Phys.* **95**, 7880 (1991).
- <sup>63</sup>T. A. Pham, A. Daunois, J. C. Merle, J. Lemoigne, and J. Y. Bigot, *Phys. Rev. Lett.* **74**, 904 (1995).